Paclitaxel causes *de novo* induction of invasive breast cancer cells by repolarizing tumor-associated macrophages

Madeline Friedman-DeLuca,[1,2,3] George S. Karagiannis,[2,3,4,5,6] Camille L. Duran,[1,2,3] Suryansh Shukla,[1,2,3,5] Jiufeng Li,[1,3] John S. Condeelis,[2,3,5,6,7,8] Maja H. Oktay,*[1,2,3,5,6,7] David Entenberg*[1,2,3,5,6]

[1]Department of Pathology, Albert Einstein College of Medicine/ Montefiore Medical Center, Bronx, NY, USA; [2]Integrated Imaging Program for Cancer Research, Albert Einstein College of Medicine/ Montefiore Medical Center, Bronx, NY, USA; [3]Cancer Dormancy Institute, Albert Einstein College of Medicine/ Montefiore Medical Center, Bronx, NY, USA; [4]Department of Microbiology and Immunology, Albert Einstein College of Medicine/ Montefiore Medical Center, Bronx, NY, USA; [5]Gruss-Lipper Biophotonics Center, Albert Einstein College of Medicine/ Montefiore Medical Center, Bronx, NY, USA; [6]Tumor Microenvironment and Metastasis Program, Albert Einstein College of Medicine/ Montefiore Medical Center, Bronx, NY, USA; [7]Department of Surgery, Albert Einstein College of Medicine/ Montefiore Medical Center, Bronx, NY, USA [8]Department of Cell Biology, Albert Einstein College of Medicine/ Montefiore Medical Center, Bronx, NY, USA.

*Corresponding authors

Keywords: Breast cancer, macrophages, MenaINV, NF-κB, Notch1

Abstract

Background: Metastasis is the leading cause of breast cancer (BC) death, and tumor cells must migrate and invade to metastasize. BC cells that express the pro-metastatic actin regulatory protein MenaINV have an enhanced ability to migrate and intravasate within the primary tumor and extravasate at secondary sites. Though chemotherapy improves patient survival, treatment with paclitaxel leads to upregulation of MenaINV and an increase in metastasis in mice. MenaINV expression can be induced in BC cells through cooperative NF-κB/ Notch1 signaling with macrophages, which are often increased in tumors in response to chemotherapy. MenaINV-expressing cells are also resistant to paclitaxel, begging the question of whether paclitaxel increases MenaINV by *de novo* induction or by selectively killing non-MenaINV-expressing cells. We hypothesized that paclitaxel causes *de novo* MenaINV induction by increasing macrophage-tumor cell NF-κB/ Notch1 signaling. Understanding this pro-metastatic effect of chemotherapy is crucial to refining treatment strategies.

Findings: Paclitaxel-treated tumors expressed significantly more MenaINV than vehicle-treated tumors. This effect was dependent upon both macrophages and NF-κB/ Notch signaling. This indicates that chemotherapy increases MenaINV expression by induction. Mechanistically, paclitaxel causes macrophages to take on a pro-inflammatory phenotype and increase NF-κB/ Notch1 signaling with tumor cells.

Conclusion: Paclitaxel causes *de novo* MenaINV induction. Mechanistically, paclitaxel repolarizes tumor-associated macrophages towards a pro-inflammatory phenotype. These pro-inflammatory macrophages then participate in enhanced NF-κB/ Notch1 signaling with tumor cells, which leads to MenaINV induction in the tumor cells. These results lay the groundwork for novel microenvironment-based therapies to alleviate the pro-metastatic effects of chemotherapy in BC.

43 **Introduction**

44 Breast cancer (BC) is the second leading cause of cancer death among women in the
45 United States, and the majority of these deaths are due to metastasis (1). To metastasize, tumor
46 cells must be able to migrate and intravasate within the primary tumor and extravasate at
47 secondary sites. Tumor cells perform these tasks using invadopodia – actin-rich protrusions with
48 proteolytic activity that degrade surrounding extracellular matrix, forging a path for the cell. In BC
49 cells, the actin regulatory protein MenaINV (Mammalian enabled, invasive variant) supports
50 invadopodium stability and degradative activity (2), making cells more migratory and metastatic.
51 Furthermore, tumor cells that express MenaINV are more sensitive to chemotactic gradients in
52 the tumor microenvironment, which facilitate invadopodium formation and directional migration
53 towards blood vessels where they intravasate (3, 4). Indeed, BC cells that express MenaINV have
54 an enhanced ability to migrate, intravasate, and extravasate (4-6), and high MenaINV expression
55 is associated with poor outcomes in both mouse and human BC (4, 7).

56 Though chemotherapy improves patient survival, treatment with neoadjuvant paclitaxel
57 increases the proportion of MenaINV-expressing cells in both mouse and human residual breast
58 tumors, as well as lung metastasis in mice (8). MenaINV-expressing cells are resistant to
59 paclitaxel (9), so the observed increase in MenaINV after paclitaxel treatment may be due to the
60 selective killing of non-MenaINV-expressing cells. However, we have also shown that MenaINV
61 is induced in tumor cells via cooperative NF-κB/ Notch1 signaling with macrophages (10).
62 Chemotherapy has been shown to cause a macrophage influx into tumors in response to tissue
63 damage, potentially increasing macrophage-tumor cell NF-κB/ Notch1 signaling and MenaINV
64 induction. This means that, in addition to the selective killing of non-MenaINV-expressing cells,
65 paclitaxel may also cause *de novo* induction of MenaINV in cells that did not previously express
66 it. We hypothesized that paclitaxel induces MenaINV expression by increasing macrophage
67 infiltration and macrophage-tumor cell NF-κB/ Notch1 signaling. Here, we find that paclitaxel

68 causes macrophages to adopt a pro-inflammatory phenotype that promotes NF-κB/ Notch1

69 signaling and leads to *de novo* induction of MenaINV in tumor cells.

70 **Results**

71 Paclitaxel causes *de novo* induction of MenaINV

72 To test whether paclitaxel causes *de novo* MenaINV induction, we treated FVB-PyMT mice
73 bearing spontaneous breast tumors with paclitaxel and co-administered either DAPT – to prevent
74 MenaINV induction (10, 11) – or vehicle control (**Fig. 1A**). DAPT is a γ-secretase inhibitor that is
75 traditionally used to block Notch signaling. However, given the significant crosstalk between the
76 Notch and NF-κB pathways, we (10) and others (12) have found that DAPT effectively inhibits
77 NF-κB activation as well. If paclitaxel increases MenaINV only by selection, we would expect that
78 dual DAPT/ paclitaxel treatment would result in the same increase in MenaINV as treatment with
79 paclitaxel alone through the selective killing of non-MenaINV-expressing cells.

80 Following treatment, mice were sacrificed, and their tumors were analyzed for MenaINV
81 expression, Notch1 activation (measured by the expression of cleaved Notch1 intracellular
82 domain), NF-κB activation (measured by p65 nuclear localization), and macrophage infiltration.
83 As previously observed, tumors from mice treated with paclitaxel expressed significantly more
84 MenaINV than the control group (**Fig. 1B**), and this was accompanied by a significant increase in
85 Notch1 and NF-κB activation (**Fig. 1C, D**). When MenaINV induction was inhibited with DAPT,
86 paclitaxel no longer caused an increase in MenaINV expression (**Fig. 1E**). This indicates that
87 paclitaxel causes *de novo* MenaINV induction.

88 We originally hypothesized that the paclitaxel-mediated MenaINV induction was due to an
89 increase in macrophage infiltration following paclitaxel treatment, but no difference in macrophage
90 infiltration was observed in any treatment group (**Fig. 1F**). This led us to question the necessity
91 of macrophages in paclitaxel-mediated MenaINV induction.

92

93 Macrophages are required for paclitaxel-mediated MenaINV induction

94 To clarify the role of macrophages in paclitaxel-mediated MenaINV induction, we treated

95 FVB-PyMT mice bearing spontaneous breast tumors with paclitaxel and co-administered
96 clodronate liposomes – to deplete macrophages – or PBS control liposomes (**Fig. 2A**). Following
97 the treatment period, the mice were sacrificed, and their tumors were analyzed for MenaINV
98 expression, Notch1 and NF-κB activation, and macrophage infiltration. Paclitaxel again caused a
99 significant induction of MenaINV, and this induction was prevented when macrophages were
100 depleted (**Fig. 2B, C**). This indicates that macrophages *are* required for paclitaxel to induce
101 MenaINV. Notch1 and NF-κB signaling were also significantly decreased upon macrophage
102 depletion (**Fig. 2D, E**), indicating that macrophages are the primary source of additional Notch1
103 and NF-κB stimulation in the tumor microenvironment following paclitaxel treatment. Our data
104 indicate that for paclitaxel to induce MenaINV, macrophages must be present, but not necessarily
105 in higher proportions than in untreated conditions. This led us to ask whether paclitaxel changes
106 the phenotype of macrophages to promote NF-κB/ Notch1 signaling.
107
108 <u>Paclitaxel induces pro-inflammatory phenotype in macrophages that promotes NF-κB/ Notch1</u>
109 <u>signaling</u>
110 To investigate how paclitaxel affects the ability of macrophages to participate in NF-κB/
111 Notch1 signaling, we cultured RAW264.7 murine macrophages with paclitaxel (0 μM, 10 μM, and
112 30 μM) for 24 h and measured the levels of secreted TNFα, IL-1β, and TGF-β1, which are known
113 to directly activate NF-κB. TGF-β1 has also been shown to enhance Notch signaling in several
114 contexts (13, 14). Treatment with paclitaxel significantly increased macrophage secretion of all
115 three cytokines (**Fig. 3A, B, C**). These effects were not dose-dependent at the tested
116 concentrations.
117
118 <u>Paclitaxel repolarizes macrophages in patients treated with neoadjuvant chemotherapy</u>
119 We next sought to establish supporting evidence that chemotherapy causes a

120 repolarization of primary tumor macrophages in patients, and to confirm the clinical relevance of
121 this finding. To do this, we identified a previously published dataset of single-cell RNA sequencing
122 reads from biopsies from human BC patients taken either before receiving any treatment
123 (treatment naïve) or after receiving neoadjuvant chemotherapy (NAC), as described in the original
124 publication (15). We analyzed the macrophage compartment of this dataset and found that
125 macrophages cluster into 4 major groups (0-3), and one minor group (4) (**Fig. 3D**) which express
126 gene signatures that are associated with either NF-κB activation/inflammatory response (e.g.
127 TNFα, TGF-β, and IL-6) (referred to here as M1), or anti-inflammatory phenotypes with markedly
128 lower inflammatory pathway activation (referred to here as M2), or a mixture of the two (**Fig. 3E**),
129 as previously published (16). By including these three categories, our analysis accounts for a
130 spectrum of macrophage polarizations, rather than imposing a dichotomy. Under chemotherapy,
131 clusters 1 & 3 (M1 and mixed, respectively) dominate, with the M1 cluster accounting for 75% of
132 macrophages. Meanwhile, clusters 0 & 2 (mixed and M2, respectively) dominate under naïve
133 conditions (**Fig. 3F**). Population analysis of the clusters shows a dramatic increase in the M1
134 cluster 1 and mixed cluster 3 after chemotherapy (**Fig. 3G**). Pathway analysis shows that,
135 compared to clusters 0 & 2, cluster 1 is higher in TNFα and TGF-β signaling, and cluster 3 is
136 higher in TGF-β signaling (**Fig. 3H**). These results confirm that NAC promotes an inflammatory
137 phenotype in macrophages in human BC, which increases their ability to participate in NF-κB/
138 Notch1 signaling, and complement our previous finding that NAC increases MenaINV expression
139 in human BC (8).

140 Taken together, our results reveal that chemotherapy skews macrophages from an anti-
141 inflammatory/M2 phenotype towards a pro-inflammatory/M1 phenotype, increasing their ability to
142 participate in NF-κB/ Notch1 signaling and subsequent MenaINV induction (**Fig. 4**).

143 **Discussion**

144 In this study, we discovered that neoadjuvant paclitaxel induces the expression of the pro-
145 metastatic protein MenaINV in BC cells by promoting NF-κB/ Notch1 signaling with macrophages.
146 We previously found that paclitaxel causes an increase in MenaINV (8, 10). However, given that
147 MenaINV expression confers resistance to paclitaxel (9), it was unknown whether the observed
148 increase was a result of *de novo* induction or the selective killing of non-MenaINV-expressing
149 cells. Here, we show that the increase in MenaINV following paclitaxel treatment is the result of
150 *de novo* induction. When the pathways involved in MenaINV induction were blocked during
151 paclitaxel treatment, no increase in MenaINV expression was observed (**Fig. 1E**). These results
152 indicate that paclitaxel induces MenaINV expression.

153 We have previously shown that Notch1 signaling between macrophages and tumor cells
154 is crucial for robust MenaINV induction (10, 11). The Notch1 receptor and its ligands are
155 membrane-bound, so Notch1 signaling only occurs between adjacent cells. Given this, and our
156 previous finding that macrophages play a key role in the paclitaxel-mediated increase in MenaINV
157 (10), we hypothesized that paclitaxel causes a macrophage influx into the tumor, increasing the
158 potential for macrophage-tumor cell Notch1 signaling by increasing the number of tumor cells in
159 direct contact with macrophages. Interestingly, we found that, while macrophages are necessary
160 for paclitaxel to induce MenaINV expression (**Fig. 2B**), an increase in macrophage proportion is
161 not (**Fig. 1E, F**). We conclude that, rather than increasing macrophage-tumor cell NF-κB/ Notch1
162 signaling by increasing macrophage infiltration, paclitaxel repolarizes macrophages, allowing
163 them to participate in such signaling more readily (**Fig. 3**). This is consistent with previous reports
164 that paclitaxel activates TLR4 receptors on macrophages, leading to an increase in inflammatory
165 signaling (17).

166 Chemotherapy has long been known to exert both pro- and anti-tumoral effects on
167 macrophages, and an existing body of evidence shows that chemotherapy-induced pro-

168 inflammatory macrophages are part of the anti-tumoral response (18). Indeed, an increase in pro-
169 inflammatory macrophages following chemotherapy has been linked with an elevated innate and
170 adaptive anti-tumoral immune response (18). In the present study, we provide evidence that
171 chemotherapy-induced pro-inflammatory macrophages also have the pro-tumoral effect of
172 increasing the expression of the pro-metastatic protein MenaINV. As drug discovery platforms and
173 the ability to target specific proteins improve, it is crucial to continue deeper investigations into
174 the exact mechanisms behind both the pro- and anti-tumoral responses to chemotherapy to
175 continue refining treatment strategies.

176 **Materials & Methods**

177 Animal models

178 All procedures were performed in accordance with National Institutes of Health regulations
179 and approved by the Albert Einstein College of Medicine Institutional Animal Care and Use
180 Committee. Transgenic mice expressing the polyoma virus middle-T (PyMT) antigen under the
181 control of the mouse mammary tumor virus long terminal repeat (MMTV-LTR) (19) were bred in
182 house and have palpable mammary tumors at approximately 6 weeks of age. Only female mice
183 were used in experiments.

184

185 *In vivo* treatments

186 Treatments began when mice were 8-10 weeks of age. Paclitaxel (Sigma) was
187 reconstituted to a stock concentration of 10 mg/mL in 1:1 ethanol/Cremophor-EL (Millipore Sigma
188 238470) and stored in aliquots at -20 °C. Immediately before treatments, the stock solution was
189 further diluted in PBS and given at a dose of 10 mg/kg intravenously (total injected volume 200
190 μL) for a total of 3 doses 5 days apart. Mice in the vehicle control groups received the same
191 volume of ethanol/Cremophor-EL diluted in PBS on the same schedule.

192 DAPT (Sigma D5942) was reconstituted in 100% ethanol to a stock concentration of 20
193 mg/mL and stored in aliquots at -20 °C. Immediately before treatments, the stock solution was
194 further diluted in corn oil and given at a dose of 10 mg/kg intraperitoneally (total injected volume
195 100 μL) daily for 14 days. Mice in the vehicle control groups received the same volume of ethanol
196 in corn oil on the same schedule.

197 Clodronate liposomes (Encapsula Nano Sciences, SKU# CLD-8901) or PBS control
198 liposomes were stored at 4 °C. Mice received 200 μL liposomes (concentration 18.4 mM)
199 intraperitoneally every 2 days for 14 days.

200

201 Tissue fixing and staining

202 Following treatments, mice were sacrificed, and mammary tumors were removed and
203 fixed in 10% formalin for 24-48 hours (tumor to formalin volume ratio of 1:7). Tissues were then
204 paraffin-embedded and cut in 5 μm thick sections. Slides were deparaffinized by melting the
205 paraffin at 60 °C for 1 h, followed by 2 x 10-min incubations in xylene. Slides were then rehydrated
206 in ethanol and water, and antigen retrieval was performed in 1x citrate buffer (pH 6.0, Vector
207 H3300) at 97 °C for 20 min in a steamer.

208 For cleaved Notch1 intracellular domain (cN1ICD) and p65 staining, slides were then
209 incubated in 0.3% hydrogen peroxide in water for 10 min to quench endogenous peroxidase and
210 then blocked in a buffer containing 1% bovine serum albumin, 1% normal goat serum, and 10%
211 fetal bovine serum (FBS) in 0.05% PBS-Tween20 for 1 h at room temperature. Slides were then
212 stained using the multiplex tyramide signal amplification (TSA) immunofluorescence assay
213 (Akoya Biosciences) according to the manufacturer's instructions with the following primary
214 antibodies: rabbit anti-cN1ICD (1:200, CST4147), rabbit anti-p65 (1:4000, CST8242). Briefly,
215 slides were incubated in the appropriate primary antibody diluted in blocking buffer overnight at 4
216 °C. The next day, slides were washed 3 x 5 min in 0.5% PBS-Tween20 and then incubated in
217 goat anti-rabbit-HRP diluted 1:2000 in blocking buffer for 1 h at room temperature. After washing
218 3 x 5 min with 0.5% PBS-Tween20, TSA was performed by incubating slides in Opal reagents
219 (Akoya FP1487001KT and FP1496001KT) diluted 1:100 in amplification buffer for exactly 9 min.
220 The process of antigen retrieval, blocking, antibody incubation, and TSA was repeated for each
221 primary antibody. After the final wash, slides were incubated in DAPI for 5 min and mounted with
222 ProLong Diamond Antifade Mountant (Invitrogen).

223 For MenaINV and IBA1 staining, following antigen retrieval, slides were incubated in
224 blocking buffer (same as above) for 1 h at room temperature. The tissues were then incubated in
225 the following primary antibodies diluted in blocking buffer overnight at 4 °C: chicken anti-MenaINV

226 (0.25 μg/mL, generated by Covance as previously described (11)), rat anti-IBA1 (1:800, Invitrogen
227 MA5-38266). The next day, slides were washed 3 x 5 min in 0.05% PBS-Tween20 and incubated
228 in the following secondary antibodies diluted in blocking buffer for 1 h at room temperature: goat
229 anti-chicken 555 (1:250, Invitrogen A32932), goat anti-rat 647 (1:1000, Invitrogen A21247). After
230 washing 3 x 5 min in 0.05% PBS-Tween20, slides were incubated in DAPI for 5 minutes and
231 mounted using ProLong Diamond Antifade Mountant (Invitrogen). All stained slides were imaged
232 on the Pannoramic 250 Flash II digital whole slide scanner using a 20 x 0.75NA objective lens.
233
234 Image analysis
235 To analyze the % MenaINV+ area and % IBA1+ area, the digital whole slide scans of slides
236 stained for MenaINV and IBA1 were uploaded into CaseViewer (3DHISTECH), and 10 different
237 40X fields of view representative of the entire tumor were chosen for each mouse from invasive,
238 non-necrotic areas of the tumor. Tif files of each field of view were acquired and uploaded to FIJI
239 (NIH). In FIJI, images were thresholded based on the negative staining control, and the area
240 fraction (area of signal/total area of field) was calculated in each channel for each field of view.
241 The average value of the 10 fields per mouse is reported.
242 To analyze Notch1 activation, the digital whole slide scans of slides stained for cN1ICD
243 were uploaded into CaseViewer, and representative fields of view were chosen and uploaded to
244 FIJI as described above. In FIJI, images were thresholded based on the negative staining control.
245 The area of cN1ICD signal was normalized to the total DAPI area in each field, and the average
246 value of the 10 fields per mouse is reported.
247 To analyze NF-κB activation via p65 nuclear localization, the digital whole slide scans of
248 slides stained for p65 were uploaded into CaseViewer, and representative fields of view were
249 chosen and uploaded to FIJI as described above. In FIJI, images were thresholded based on the
250 negative staining control, and two masks were made - one of the total p65 signal and one of the

251 DAPI signal. P65 was considered nuclear if it overlapped with a DAPI-stained nucleus. Nuclear
252 p65 was normalized to the total DAPI signal in the field, and the average value of the 10 fields per
253 mouse is reported.
254
255 Enzyme-linked immunosorbent assay (ELISA)
256 Paclitaxel used in the cell culture (ThermoFisher J62734.MC) was reconstituted in DMSO
257 at a stock concentration of 0.01 M and stored in aliquots at -20 °C.
258 In the morning, RAW264.7 cells were seeded at a density of 7.5 x 10^5 cells/well in a 6-well
259 plate in DMEM containing 10% FBS and 1% penicillin/streptomycin. That evening, the media was
260 replaced with serum-starving DMEM (1% FBS, 1% penicillin/streptomycin). The cells were serum-
261 starved overnight. The next morning, the media was replaced with fresh serum-starving media
262 with the indicated concentrations of paclitaxel. Conditioned media from the cultured cells were
263 collected after 24 h and stored at -80 °C until use. Levels of TNFα, IL-1β, and TGF-β1 were
264 determined using ELISA kits (R&D Systems) according to the manufacturer's instructions. The
265 concentrations of secreted proteins were interpolated from the standard curve measurements.
266
267 Single-cell RNA sequencing analysis
268 Single-cell RNA sequencing data was obtained from the publicly available site
269 http://biokey.lambrechtslab.org. Raw sequencing reads can also be found in the European
270 Genome-phenome Archive under study number EGAS00001004809 (15). Only cells taken from
271 biopsies before anti-PD1 therapy ("Pre" condition) were considered in our analysis.
272 *Quality control and dimensionality reduction:* As the archived dataset had already been
273 subjected to rigorous quality control measures by the original authors, no additional quality control
274 measures needed to be performed. Raw counts were normalized using the Seruat
275 "NormalizeData" function, and principal component analysis (PCA) was performed to reduce the

276 dimensionality of the data and mitigate potential batch effects. Harmony integration was
277 subsequently applied using the PCA embeddings as input.

278 *Cell type annotation:* Cell types were annotated using the SingleR package, as previously
279 described (16).

280 *Clustering:* Cells were clustered using the Seurat framework. PCA and Harmony reduction
281 were employed to derive a low-dimensional representation of the data, followed by the
282 identification of neighbors and clusters using Seurat's FindNeighbors and FindClusters functions.
283 A resolution of 0.3 was used to balance cluster granularity. Clusters were visualized using Uniform
284 Manifold Approximation and Projection (UMAP) for high-dimensional data.

285 *Gene set variation analysis (GSVA):* GSVA was performed using the GSVA R package to
286 evaluate pathway activity across the dataset. Gene sets were sourced from the Molecular
287 Signatures Database (MSigDB). GSVA was parallelized using the BiocParallel package. Pathway
288 activity was summarized for each cluster by calculating the mean enrichment scores for each
289 pathway across cells in the cluster. Differential gene expression analysis was performed between
290 the identified clusters.

291 *Macrophage marker analysis:* Macrophages were categorized into three classes: M1, M2,
292 or mixed M1/M2 based on literature-reported markers, as previously described (16). The M1
293 markers used were CD80, CD86, IRF3, IRF5, STAT1, and STAT5. The M2 markers used were
294 STAT3, STAT6, IRF4, KLF4, JMJD3, CD163, CD206, and CD209.

295

296 **Figure Legends**

297 **Figure 1**: (**A**) Experimental design of paclitaxel (ptx) and DAPT treatments in PyMT mice. (**B**) %
298 MenaINV+ area in control (ctrl)- and paclitaxel-treated tumors. (**C**) Notch1 activation in control-
299 and paclitaxel-treated tumors. (**D**) NF-kB activation in control- and paclitaxel-treated tumors. (**E**)
300 % MenaINV+ area in tumors treated with control, paclitaxel, and paclitaxel + DAPT. (**F**)
301 Macrophage infiltration (% IBA1+ area) in tumors treated with control, paclitaxel, and paclitaxel +
302 DAPT.

303

304 **Figure 2**: (**A**) Experimental design of paclitaxel and clodronate (cld) treatments in PyMT mice. (**B**)
305 % MenaINV+ area in tumors treated with control, paclitaxel, and paclitaxel + clodronate. (**C**)
306 Macrophage infiltration (# IBA1+ cells per high power field (HPF) in tumors treated with control,
307 paclitaxel, and paclitaxel + clodronate. (**D**) Notch1 activation in tumors treated with control,
308 paclitaxel, and paclitaxel + clodronate. (**E**) NF-kB activation in tumors treated with control,
309 paclitaxel, and paclitaxel + clodronate.

310

311 **Figure 3**: Secretion of (**A**) TNAα, (**B**) IL-1β, and (**C**) TGF-β1 from RAW264.7 macrophages treated
312 with paclitaxel. (**D-H**) scRNAseq analysis of macrophages in the tumors of breast cancer patients
313 who were treatment naïve or had undergone neoadjuvant chemotherapy. (**D**) Clustering analysis
314 showing 4 major groups (0-3), and one minor group (4). (**E**) Clusters correlated with signatures
315 indicative of M1, M2 or mixed types. (**F**) M1 cluster 1 & mixed cluster 3 dominate under
316 chemotherapy; mixed cluster 0 & M2 cluster 2 dominate under naïve conditions. (**G**)
317 Chemotherapy results in a dramatic increase in M1 cluster 1 & mixed cluster 3. (**H**) Pathway
318 analysis shows that, compared to clusters 0 & 2, cluster 1 is higher in TNFα & TGF-β signaling
319 (green boxes), and cluster 3 is higher in TGF-β signaling.

320

321 **Figure 4**: Paclitaxel induces MenaINV expression in tumor cells by skewing macrophages from
322 a mixed/M2 (anti-inflammatory) phenotype to a mixed/M1 (pro-inflammatory) phenotype that
323 increasingly activates Notch1 and NF-kB signaling in tumor cells, leading to increased MenaINV
324 expression.

Declarations

Ethics approval and consent to participate

All procedures were conducted in accordance with National Institutes of Health regulations and approved by the Albert Einstein College of Medicine Institutional Animal Care and Use Committee.

Consent for publication

Not applicable

Availability of data and materials

The datasets used and/or analyzed during the current study are available from the corresponding author on reasonable request.

Competing interests

The authors declare that they have no competing interests.

Funding

This study was supported by grants from the NIH (R01 CA255153, K99/R00 CA237851), SIG OD019961, the Gruss-Lipper Biophotonics Center, the Integrated Imaging Program for Cancer Research, The Evelyn Gruss-Lipper Charitable Foundation, and The Helen & Irving Spatz Foundation.

Authors' contributions

MFD, MHO, and DE performed conceptualization. MFD, GSK, CLD, SS, and JL provided methodology. MFD and JL carried out formal analysis. SS & DE provided software and computational image analysis. MFD, GSK, and CLD performed investigation. MFD wrote the

manuscript. GSK, JSC, MHO, and DE performed funding acquisition. MHO and DE supervised the study. All authors read and approved the final manuscript.

Acknowledgments

We thank the Histopathology Core Facility for their assistance with sample processing and the Analytical Imaging Facility for their imaging services. We thank Robert Eddy for the development and validation of the MenaINV antibody. We thank Luis Rivera Sanchez for assistance with macrophage quantification and Ved Sharma for contributing to sample generation. We thank Shanye Yin and Erqiang Hu for providing their scRNAseq macrophage analysis code.

359 **References**

360 1. Siegel RL, Giaquinto AN, Jemal A. Cancer statistics, 2024. CA Cancer J Clin. 2024;74(1).

361 2. Weidmann MD, Surve CR, Eddy RJ, Chen X, Gertler FB, Sharma VP, et al. MenaINV
362 dysregulates cortactin phosphorylation to promote invadopodium maturation. Sci Rep.
363 2016;6:36142.

364 3. Hughes SK, Oudin MJ, Tadros J, Neil J, Del Rosario A, Joughin BA, et al. PTP1B-
365 dependent regulation of receptor tyrosine kinase signaling by the actin-binding protein Mena. Mol
366 Biol Cell. 2015;26(21):3867-78.

367 4. Philippar U, Roussos ET, Oser M, Yamaguchi H, Kim HD, Giampieri S, et al. A Mena
368 invasion isoform potentiates EGF-induced carcinoma cell invasion and metastasis. Dev Cell.
369 2008;15(6):813-28.

370 5. Goswami S, Philippar U, Sun D, Patsialou A, Avraham J, Wang W, et al. Identification of
371 invasion specific splice variants of the cytoskeletal protein Mena present in mammary tumor cells
372 during invasion in vivo. Clin Exp Metastasis. 2009;26(2):153-9.

373 6. Borriello L, Coste A, Traub B, Sharma VP, Karagiannis GS, Lin Y, et al. Primary tumor
374 associated macrophages activate programs of invasion and dormancy in disseminating tumor
375 cells. Nat Commun. 2022;13(1):626.

376 7. Oudin MJ, Jonas O, Kosciuk T, Broye LC, Guido BC, Wyckoff J, et al. Tumor Cell-Driven
377 Extracellular Matrix Remodeling Drives Haptotaxis during Metastatic Progression. Cancer Discov.
378 2016;6(5):516-31.

379 8. Karagiannis GS, Pastoriza JM, Wang Y, Harney AS, Entenberg D, Pignatelli J, et al.
380 Neoadjuvant chemotherapy induces breast cancer metastasis through a TMEM-mediated
381 mechanism. Sci Transl Med. 2017;9(397).

382 9. Oudin MJ, Barbier L, Schafer C, Kosciuk T, Miller MA, Han S, et al. MENA Confers
383 Resistance to Paclitaxel in Triple-Negative Breast Cancer. Mol Cancer Ther. 2017;16(1):143-55.

384 10. Duran CL, Karagiannis GS, Chen X, Sharma VP, Entenberg D, Condeelis JS, et al.
385 Cooperative NF-kappaB and Notch1 signaling promotes macrophage-mediated MenaINV
386 expression in breast cancer. Breast Cancer Res. 2023;25(1):37.
387 11. Pignatelli J, Bravo-Cordero JJ, Roh-Johnson M, Gandhi SJ, Wang Y, Chen X, et al.
388 Macrophage-dependent tumor cell transendothelial migration is mediated by Notch1/MenaINV-
389 initiated invadopodium formation. Sci Rep. 2016;6:37874.
390 12. Li LH, Hsu DZ, Chandrasekaran VRM, Liu MY. Inhibiting CD44-ICD Attenuates LPS-
391 Induced Initiation of Hepatic Inflammation in Septic Mice. Int J Mol Sci. 2024;25(16).
392 13. Wang Y, Shen RW, Han B, Li Z, Xiong L, Zhang FY, et al. Notch signaling mediated by
393 TGF-beta/Smad pathway in concanavalin A-induced liver fibrosis in rats. World J Gastroenterol.
394 2017;23(13):2330-6.
395 14. Blokzijl A, Dahlqvist C, Reissmann E, Falk A, Moliner A, Lendahl U, et al. Cross-talk
396 between the Notch and TGF-beta signaling pathways mediated by interaction of the Notch
397 intracellular domain with Smad3. J Cell Biol. 2003;163(4):723-8.
398 15. Bassez AA-O, Vos H, Van Dyck L, Floris GA-O, Arijs IA-OX, Desmedt CA-O, et al. A single-
399 cell map of intratumoral changes during anti-PD1 treatment of patients with breast cancer. (1546-
400 170X (Electronic)).
401 16. Huang Y, Wu G, Bi G, Cheng L, Liang J, Li M, et al. Unveiling chemotherapy-induced
402 immune landscape remodeling and metabolic reprogramming in lung adenocarcinoma by scRNA-
403 sequencing. Elife. 2024;13.
404 17. Wanderley CW, Colón DF, Luiz JPM, Oliveira FF, Viacava PR, Leite CA, et al. Paclitaxel
405 Reduces Tumor Growth by Reprogramming Tumor-Associated Macrophages to an M1 Profile in
406 a TLR4-Dependent Manner. Cancer Res. 2018;78(20):5891-900.
407 18. Friedman-DeLuca M, Karagiannis GS, Condeelis JS, Oktay MH, Entenberg D.
408 Macrophages in tumor cell migration and metastasis. Front Immunol. 2024;15:1494462.

409 19. Guy CT, Cardiff RD, Muller WJ. Induction of mammary tumors by expression of
410 polyomavirus middle T oncogene: a transgenic mouse model for metastatic disease. Mol Cell Biol.
411 1992;12(3):954-61.

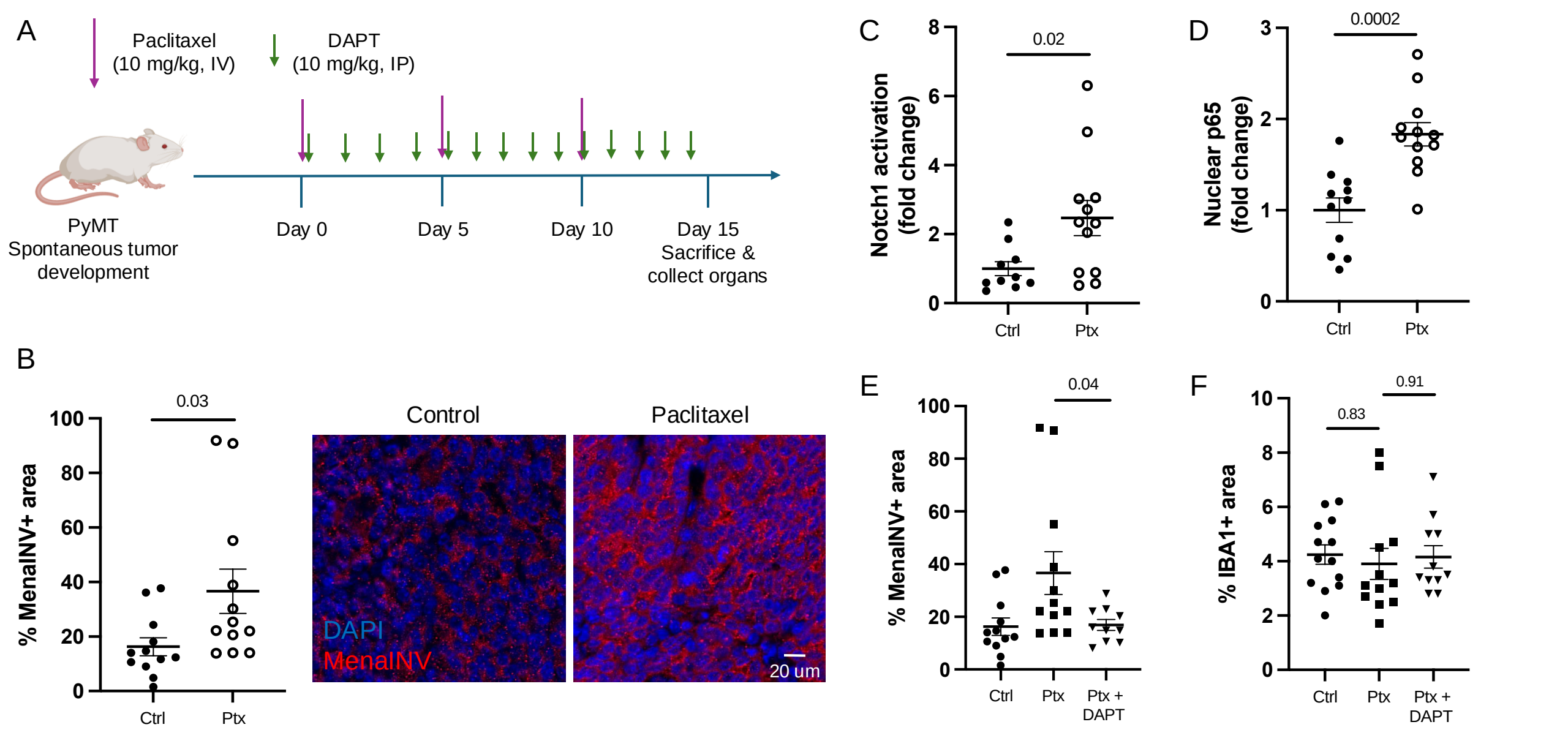
A
Paclitaxel
(10 mg/kg, IV)
DAPT
(10 mg/kg, IP)
PyMT
Spontaneous tumor
development
Day 0
Day 5
Day 10
Day 15
Sacrifice &
collect organs
B
0.03
% MenalNV+ area
Ctrl
Ptx
Control
Paclitaxel
DAPI
MenalNV
20 um
C
0.02
Notch1 activation
(fold change)
Ctrl
Ptx
D
0.0002
Nuclear p65
(fold change)
Ctrl
Ptx
E
0.04
% MenalNV+ area
Ctrl
Ptx
Ptx +
DAPT
F
0.83
0.91
% IBA1+ area
Ctrl
Ptx
Ptx +
DAPT

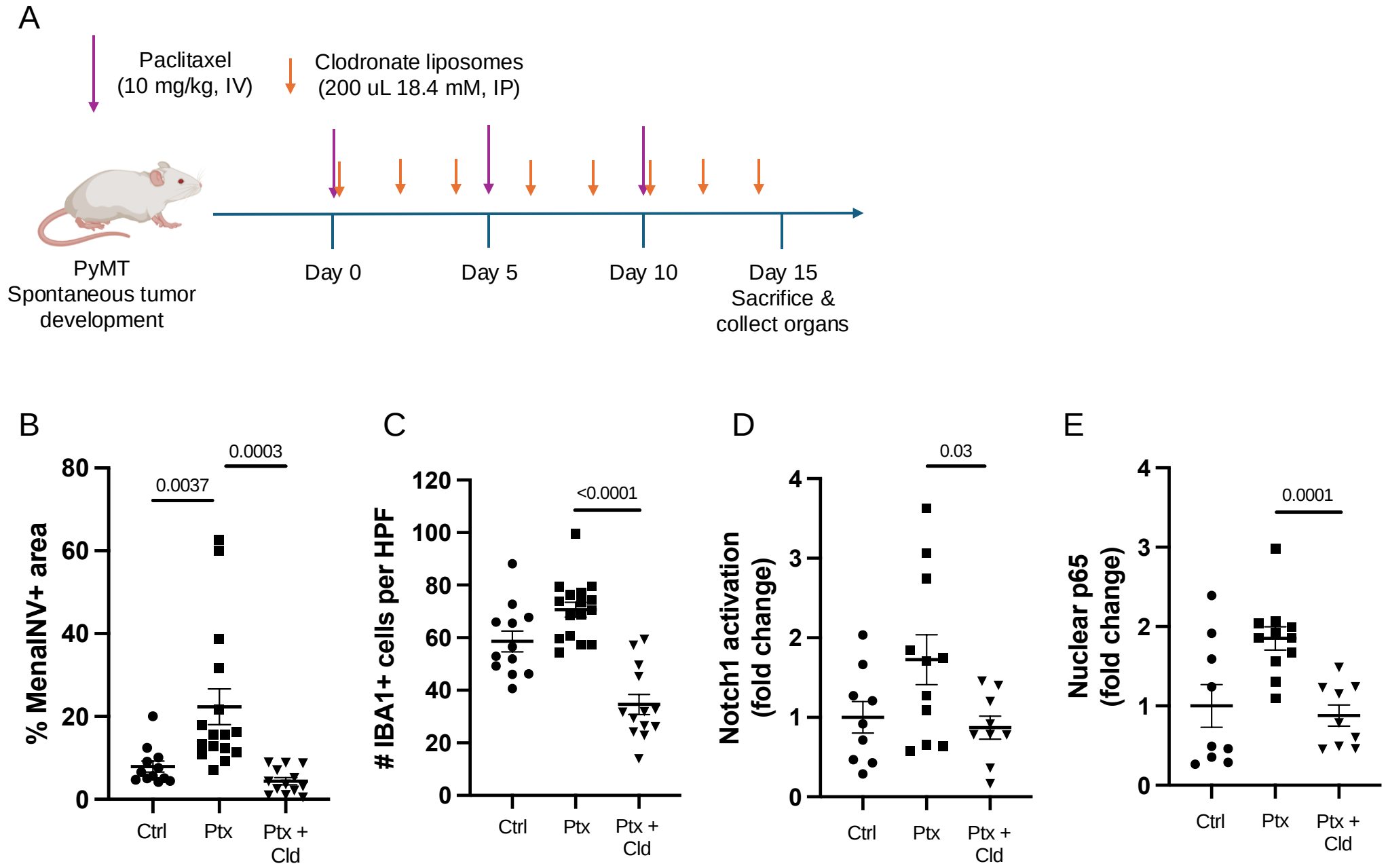
A
Paclitaxel
(10 mg/kg, IV)
Clodronate liposomes
(200 uL 18.4 mM, IP)
PyMT
Spontaneous tumor
development
Day 0
Day 5
Day 10
Day 15
Sacrifice &
collect organs
B
% MenalNV+ area
0.0037
0.0003
Ctrl
Ptx
Ptx +
Cld
C
IBA1+ cells per HPF
<0.0001
Ctrl
Ptx
Ptx +
Cld
D
Notch1 activation
(fold change)
0.03
Ctrl
Ptx
Ptx +
Cld
E
Nuclear p65
(fold change)
0.0001
Ctrl
Ptx
Ptx +
Cld

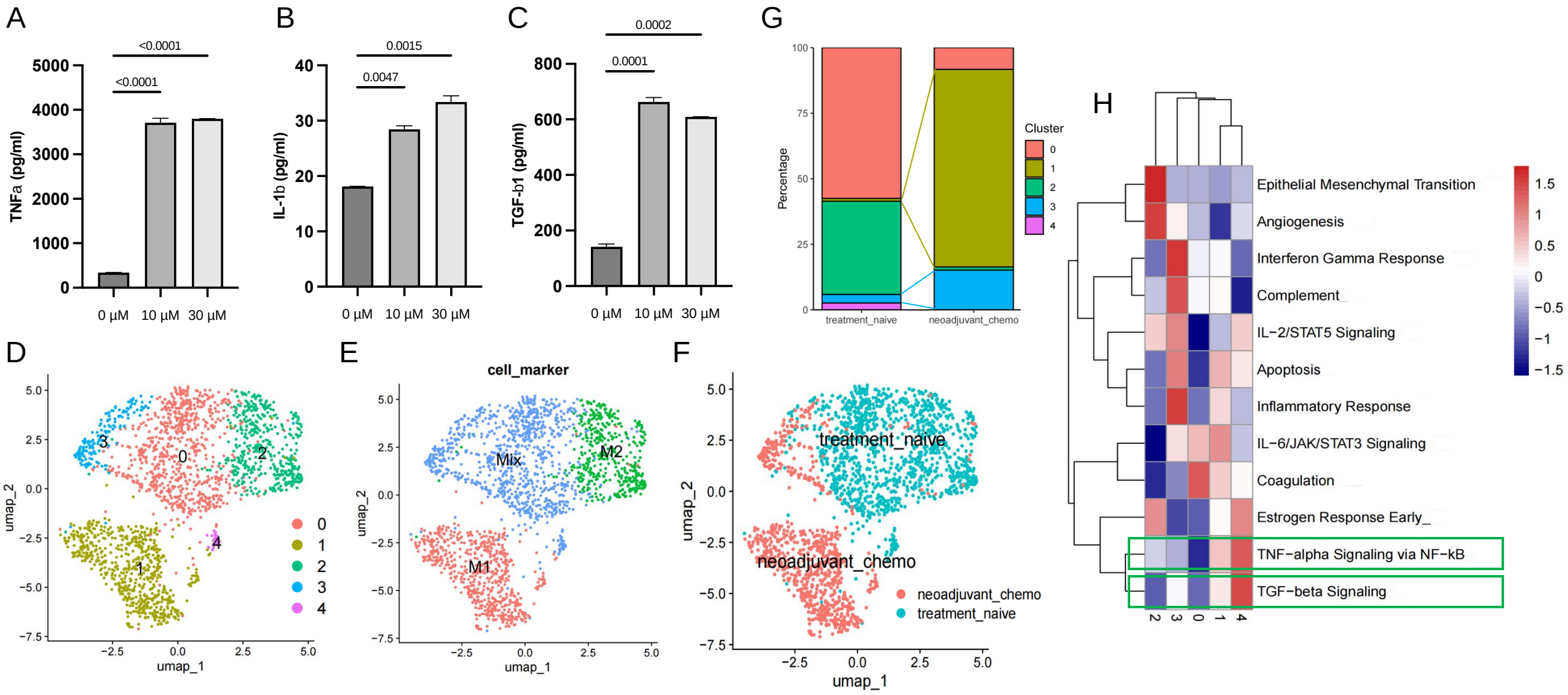
A
<0.0001
<0.0001
TNFa (pg/ml)
5000
4000
3000
2000
1000
0
0 μM
10 μM
30 μM
B
0.0015
0.0047
IL-1b (pg/ml)
40
30
20
10
0
0 μM
10 μM
30 μM
C
0.0002
0.0001
TGF-b1 (pg/ml)
800
600
400
200
0
0 μM
10 μM
30 μM
G
Percentage
100
75
50
25
0
treatment_naive
neoadjuvant_chemo
Cluster
0
1
2
3
4
H
Epithelial Mesenchymal Transition
Angiogenesis
Interferon Gamma Response
Complement
IL−2/STAT5 Signaling
Apoptosis
Inflammatory Response
IL−6/JAK/STAT3 Signaling
Coagulation
Estrogen Response Early
TNF−alpha Signaling via NF−kB
TGF−beta Signaling
2
3
0
1
4
1.5
1
0.5
0
−0.5
−1
−1.5
D
umap_1
umap_2
3
0
2
1
4
0
1
2
3
4
E
cell_marker
Mix
M2
M1
umap_1
umap_2
F
treatment_naive
neoadjuvant_chemo
neoadjuvant_chemo
treatment_naive
umap_1
umap_2

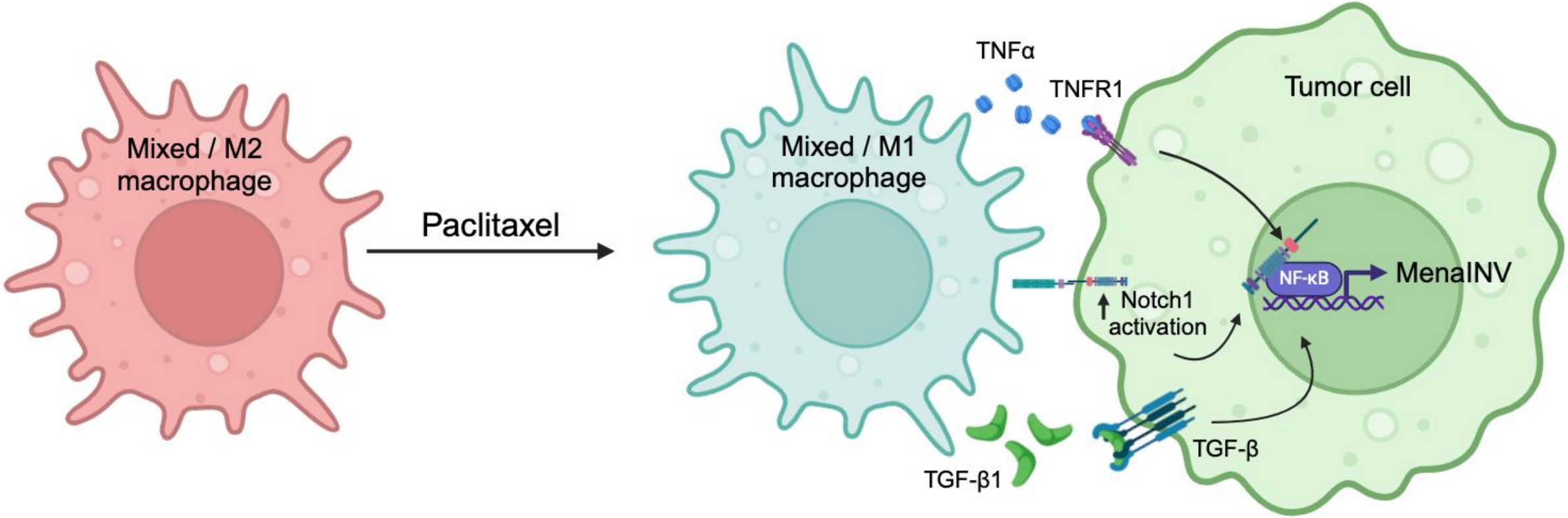
Mixed / M2
macrophage
Paclitaxel
Mixed / M1
macrophage
TNFα
TNFR1
Tumor cell
NF-κB
MenaINV
Notch1
activation
TGF-β
TGF-β1